

Fluorescent Naphthalene Diols as Bridging Ligands in Ln^{III} Cluster Chemistry: Synthetic, Structural, Magnetic, and Photophysical Characterization of Ln^{III}₈ “Christmas Stars”

Dimitris I. Alexandropoulos,[†] Adeline Fournet,[‡] Luís Cunha-Silva,[§] Andrew M. Mowson,[‡] Vlasoula Bekiari,^{||} George Christou,[‡] and Theocharis C. Stamatatos^{*,†}

[†]Department of Chemistry, Brock University, L2S 3A1 St. Catharines, Ontario, Canada

[‡]Department of Chemistry, University of Florida, Gainesville, Florida 32611-7200, United States

[§]REQUIMTE & Department of Chemistry and Biochemistry, Faculty of Sciences, University of Porto, 4169-007 Porto, Portugal

^{||}Department of Aquaculture and Fisheries Management, Technological Educational Institute of Western Greece, 30 200 Messolonghi, Greece

S Supporting Information

ABSTRACT: The initial employment of the fluorescent bridging ligand naphthalene-2,3-diol in 4f-metal coordination chemistry has provided access to a new family of Ln^{III}₈ clusters with a “Christmas-star” topology, single-molecule magnetism behavior, and ligand-centered emissions.

The field of lanthanide (Ln) coordination chemistry has received considerable attention over the past decade or so due to the ability of 4f-metal complexes to find applications in transdisciplinary areas of research, such as medicinal chemistry, optics, catalysis, and magnetism.¹ Mono- and dinuclear 4f-metal compounds have been shown to exhibit single-molecule magnetism (SMM) behaviors;² intense, long-lived emissions in the visible and near-IR regions;³ and appreciable magnetic entropy changes resulting in a new class of molecular magnetic refrigerants for low-temperature cooling applications.⁴ The crystal field environment and consequently the ligands bound to the Ln ion(s) constitute some of the most crucial factors for increasing the blocking temperatures and energy barriers for the magnetization reversal in SMMs,⁵ as well as for enhancing the optical activity of the complexes through the selection of efficient “antenna” groups.⁶ On the other hand, polynuclear 4f-metal clusters are molecular species that exhibit not only interesting physical properties, such as the ones discussed above for the mono- and dinuclear counterparts, but also aesthetically pleasing structures, unprecedented topologies and beautiful mosaics.

The combination of more than one physical property within a high nuclearity and structurally novel 4f-metal cluster is unambiguously a challenge for synthetic inorganic chemists, and the choice of the Ln ion(s) is of great importance because it directs the interest regarding the nature of the potential applications. For example, Dy^{III} and Tb^{III} are highly anisotropic and possess a significant spin, both requirements for the construction of SMMs. At the same time, Eu^{III}, Tb^{III}, and Dy^{III}-based clusters show intense photoluminescence (PL) properties with metal-centered emissions at different regions of the visible spectrum.⁷ Population of the emitting levels of the

Ln^{III} ion is best achieved by employing light-harvesting ligands that normally absorb strongly UV light and can sensitize the metal ion by intramolecular energy transfer from the ligand triplet state.^{1b,6,7}

We have recently started a program aiming at the exploration of the magneto-optical properties of polynuclear metal complexes, and the coexistence, interplay, or synergy between these dual physical properties. We decided to approach such a challenge from two different directions. First, by the *deliberate replacement* of nonemissive carboxylato ligands in known SMMs with their fluorescent analogues, without perturbing the metal-core structure and SMM properties; this approach has recently led us to the synthesis of triangular, emissive Mn^{III}₃ SMMs.⁸ The second route, the first results of which are being presented herein, involves the use of *fluorescent polyalcohol or oximate bridging ligands* by means of obtaining new polynuclear Ln^{III} metal clusters with novel topologies, SMM behaviors, and luminescent properties arising from the increased efficiency of the “antenna” fluorescent group. The organic ligand chosen was naphthalene-2,3-diol (ndH₂, Scheme S1), which has never been previously used in 4f-metal cluster chemistry.⁹

The reaction of Ln(NO₃)₃·6H₂O (Ln = Eu, Gd, Tb, and Dy), ndH₂, and Et₄NOH in a 2:1:2 molar ratio in MeCN gave pale yellow solutions that upon slow diffusion with Et₂O afforded yellowish crystals of (Et₄N)₄[Ln₈O(nd)₈(NO₃)₁₀(H₂O)₂] in 45–60% isolated yields. Representative complex (Et₄N)₄[Tb₈O(nd)₈(NO₃)₁₀(H₂O)₂]·2MeCN (3·2MeCN) was fully characterized by single-crystal X-ray crystallography, while the other analogues (Eu₈, 1; Gd₈, 2; Dy₈, 4) were identified by elemental analyses (C, H, N) and IR spectral and unit cell comparison with crystals of 3 (see the Supporting Information).

The partially labeled structure of the [Tb₈O(nd)₈(NO₃)₁₀(H₂O)₂]⁴⁻ anion of 3 is shown in Figure 1 (left). The anion of 3 has crystallographic C₁ but virtual S₄ symmetry and consists of a central [Tb₄(μ₄-O²⁻)] tetrahedron (Tb1, Tb2, Tb3, Tb4) whose four edges are each fused with the

Received: April 5, 2014

Published: May 14, 2014



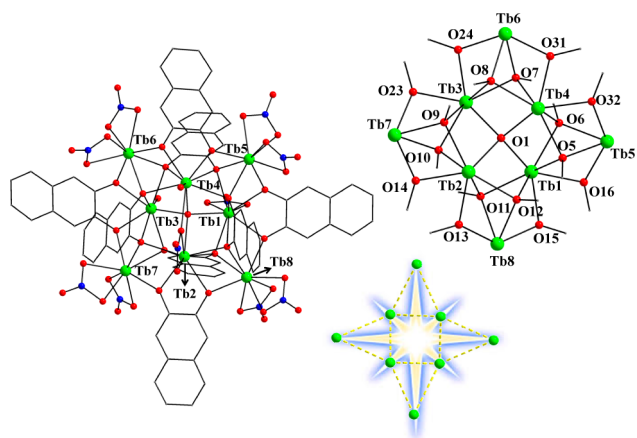


Figure 1. (Left) The structure of the anion of **3**. (Right) The $[\text{Tb}_8\text{O}(\text{OR})_{16}]^{6+}$ core of **3** emphasizing the “Christmas-star” topology. Color code: Tb^{III} , green; O, red; N, blue; C, gray.

edge of a $[\text{Tb}_3(\mu_3\text{-OR}^-)_2(\mu\text{-OR}^-)_2]$ triangle ($\text{RO}^- = \text{nd}^{2-}$). The resulting $[\text{Tb}_8(\mu_4\text{-O})(\mu_3\text{-OR})_8(\mu\text{-OR})_8]^{6+}$ core has a “Christmas-star” topology (Figure 1, right), which is unprecedented in 4f-metal cluster chemistry. Similar metal cores have been previously seen only in Fe_8 cluster chemistry, albeit with the central subcore possessing a square-planar geometry.¹⁰ In complex **3**, the central $\mu_4\text{-O}^{2-}$ (O1), whose protonation level was confirmed by oxygen BVS calculations (BVS = 2.05), is distorted tetrahedral [$\text{Tb}-\text{O}-\text{Tb} = 99.2(1)-134.7(2)^\circ$], and the $[\text{Tb}_3(\mu_3\text{-OR})_2(\mu\text{-OR})_2]^{5+}$ triangular units are essentially isosceles, the short separations [3.475(6)-3.523(6) Å] being the four (oxido)-bis(μ_3 -alkoxido)-bridged edges fused with the central tetrahedron. One of the remaining two edges of the central Tb_4 tetrahedron ($\text{Tb}2\cdots\text{Tb}4$) is additionally bridged by a $\mu\text{-O}^-$ atom (O2) from an $\eta^1:\eta^2:\mu$ NO_3^- group. In addition, each Tb^{III} of the tetrahedron is linked to two peripheral Tb^{III} atoms by two μ_3 - and two $\mu\text{-O}^-$ atoms from four $\eta^2:\eta^2:\mu_3$ and four $\eta^3:\eta^3:\mu_5$ nd^{2-} ligands (Scheme S1). The ligands possess C–O and C–C bond distances in the ranges 1.34–1.37 and 1.33–1.44 Å, respectively, which are characteristic for catecholato-type ligands rather than semi-quinonato or quinonato.¹¹ Peripheral ligation is provided by nine bidentate chelating NO_3^- groups, two on each of the external Tb^{III} atoms and the remaining on Tb1, and two H_2O molecules terminally bound to the inner Tb3 and Tb4. The internal Tb^{III} atoms are nine-coordinate, except Tb3 which is eight-coordinate; the latter coordination environment is also assigned to all external Tb^{III} atoms. To estimate the closer coordination polyhedra defined by the donor atoms around all Tb atoms in **3**, we used the program SHAPE.¹² The best fit was obtained for the muffin (Tb1), spherical capped square antiprismatic (Tb2, Tb4), square antiprismatic (Tb3, Tb5), and triangular dodecahedral (Tb6, Tb7, Tb8) geometries (Figure S1). Finally, the voids between the Tb_8 anions are occupied by counteranions and lattice solvate molecules; the crystal structure is stabilized by H bonds and interanionic $\pi-\pi$ interactions. The shortest $\text{Tb}\cdots\text{Tb}$ intermolecular distance is 9.089 Å.

Variable-temperature direct current (dc) magnetic susceptibility studies were carried out on freshly prepared, crystalline samples of complexes **1–4** in the temperature range 5.0–300 K under an applied field of 0.1 T. The obtained data for all studied compounds are shown as $\chi_{\text{M}}T$ vs T plots in Figure 2

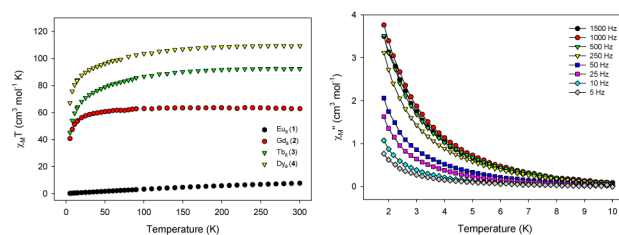


Figure 2. Plots of $\chi_{\text{M}}T$ vs T for complexes **1–4** (left) and out-of-phase (χ''_{M}) vs T ac susceptibility signals for **4** in a 3.5 G field oscillating at the indicated frequencies.

(left). The experimental $\chi_{\text{M}}T$ values at room temperature are in excellent agreement with the theoretical ones ($63 \text{ cm}^3 \text{ K mol}^{-1}$ for **2**; $94.56 \text{ cm}^3 \text{ K mol}^{-1}$ for **3**; $113.36 \text{ cm}^3 \text{ K mol}^{-1}$ for **4**) for eight noninteracting Gd^{III} ($^8\text{S}_{7/2}$, $S = 7/2$, $L = 0$, $g = 2$), Tb^{III} ($^7\text{F}_6$, $S = 3$, $L = 3$, $g = 3/2$), and Dy^{III} ($^6\text{H}_{15/2}$, $S = 5/2$, $L = 5$, $g = 4/3$) ions. For the isotropic Gd^{III} complex **2**, the $\chi_{\text{M}}T$ product remains almost constant at a value of $\sim 63 \text{ cm}^3 \text{ K mol}^{-1}$ from 300 K to ~ 80 K and then steadily decreases to a minimum value of $40.74 \text{ cm}^3 \text{ K mol}^{-1}$ at 5.0 K, indicating the presence of intramolecular antiferromagnetic exchange interactions between the eight Gd^{III} centers and/or zero-field splitting. The temperature independent behavior (300–80 K) suggests that the coupling between the Gd^{III} ions is very weak, as has been seen in many polynuclear Gd^{III} complexes. For the anisotropic Tb^{III} (**3**) and Dy^{III} (**4**) complexes, the thermal evolution of the magnetic susceptibility is very similar, in which the $\chi_{\text{M}}T$ product remains essentially constant at a value of ~ 92 and $\sim 109 \text{ cm}^3 \text{ K mol}^{-1}$ from 300 K to ~ 150 K and then rapidly decreases to a minimum value of 45.13 and $67.09 \text{ cm}^3 \text{ K mol}^{-1}$ at 5.0 K, respectively. Such a low- T decrease of the $\chi_{\text{M}}T$ product is mainly due to depopulation of the excited M_J states of the Tb^{III} and Dy^{III} ions and the weak antiferromagnetic interactions between the metal centers.^{1,2,5}

The lack of true saturation in magnetization of complexes **3** and **4** (Figures S2 and S3) indicates the presence of magnetic anisotropy and/or population of low-lying excited states. In the case of **2**, the magnetization almost reaches a saturation of $55.8 \mu_{\text{B}}$ at the highest fields (Figure S4), which is in good agreement with the expected value of $56 \mu_{\text{B}}$ for eight noncoupled Gd^{III} ions. This further supports the weak nature of the magnetic exchange interactions between the Gd^{III} ions (Figure S5) so that the antiferromagnetic interactions are easily overcome by the external field.

Alternating current (ac) magnetic susceptibility studies have also been carried out in order to investigate the magnetization dynamics of the anisotropic Tb^{III} (**3**) and Dy^{III} (**4**) clusters under a zero dc magnetic field. Complex **4** is the only member of this family of clusters which shows frequency-dependent out-of-phase χ''_{M} tails of signals at temperatures below ~ 9 K (Figure 2, right), indicative of the slow magnetization relaxation of an SMM with a small energy barrier for magnetization reversal. Such behavior most likely arises from predominant single-ion effects of the individual Dy^{III} Kramer ions within **4**.^{2,5} Given the lack of χ'' peak maxima, the energy barrier and relaxation time for **4** were approximated using a method employed by Bartolomé et al.,¹³ based on the equation $\ln(\chi''/\chi') = \ln(\omega\tau_0) + E_{\text{a}}/k_{\text{B}}T$. Considering a single relaxation process, the least-squares fits of the experimental data (Figure S7) gave an energy barrier of $\sim 1.9(2) \text{ cm}^{-1}$ ($\sim 2.8(2) \text{ K}$) and a relaxation time of $7.2(3) \times 10^{-6} \text{ s}$, consistent with the expected τ_0 values for an SMM.²

In order to gain any possible access into additional physical properties for this family of Ln_8 complexes, we decided to perform PL studies on all analogues in the solid-state and at room temperature. $\text{Ln}(\text{III})$ metal complexes have been shown to exhibit very characteristic sharp, intense, and narrow bands in their metal-centered emission spectra due to an efficient energy-transfer “sensitization” of the metal’s excited levels from the organic ligand’s triplet (or occasionally singlet) state.¹⁴ In contrast, quenching of Ln emission is relatively rare, resulting in the observation of either no emission at all or rarely a ligand-centered emission which is broad and weak. Reasons for such quenching vary and include structural factors, such as the coordination of aqua ligands and the presence of lattice solvents and counterions in the crystal,¹⁴ the temperature, as well as the location of the lowest triplet state of the ligand.¹⁴

Undoubtedly, the free ligand ndH_2 is a promising “antenna” group; upon maximum excitation at 355 nm, it shows a strong emission in the 380–450 nm range with a near-UV maximum at 394 nm (Figure 3, left), characteristic of the naphthalene

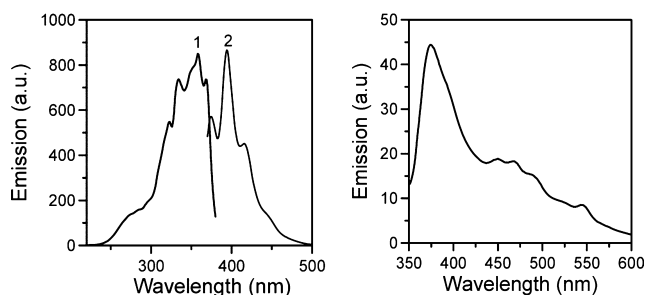


Figure 3. Excitation (1) and emission (2) spectra of solid ndH_2 (left) and complex 4 (right) at room temperature.

functional group.⁸ Such behavior offers a strong potential for successful energy transfer to the lanthanide’s excited states and consequently to a strong metal-based luminescence with small Stokes’ shifts. However, none of the complexes 1–4 showed the characteristic Ln emissions but instead similar broad and weak emissions in the range 350–600 nm (Figures 3, right, and Figure S8), upon excitation at 320 nm. Such Ln^{III} -independent luminescence is most likely attributed to a ligand-centered emission occurring through an Ln^{III} -to- nd^{2-} back energy transfer process. There is no doubt that quenching effects from the coordinated H_2O molecules, the presence of Et_4N^+ counterions and lattice solvents within 1–4, might contribute to the diminishing of the Ln^{III} emission.

In conclusion, we have shown that fluorescent, alkoxido-based bridging ligands, such as naphthalene-2,3-diol, can lead not only to unprecedented structural motifs in 4f-metal cluster chemistry but also to new SMMs and optically active materials with unusual ligand-centered emissions. We are currently trying to improve both the magnetic and optical responses of the reported compounds by combining the Ln_8 clusters with either paramagnetic and anisotropic 3d- or energy-transfer efficient metal ions (i.e., Zn^{II}), respectively.

■ ASSOCIATED CONTENT

Supporting Information

Crystallographic data (CIF format), synthesis, and various structural and magnetism figures. This material is available free of charge via the Internet at <http://pubs.acs.org>.

■ AUTHOR INFORMATION

Corresponding Author

*E-mail: tstamatatos@brocku.ca.

Notes

The authors declare no competing financial interest.

■ ACKNOWLEDGMENTS

We thank Ontario Trillium Foundation, NSERC Discovery Grant (to T.C.S.), the *Fundação para a Ciência e a Tecnologia* (FCT, Portugal) through strategic project PEst C/EQB/LA0006/2011 and the EU/FEDER/COMPETE by Operation NORTE-07-0124-FEDER-000067–Nanochemistry, and the NSF (DMR-1213030 to G.C) for funding. V.B. acknowledges financial support by the ESF and Greek national funds through the Operational Program Archimedes III.

■ REFERENCES

- (1) (a) Murugesu, M. *Nat. Chem.* **2012**, *4*, 347–348. (b) Bünzli, J.-C. G.; Eliseeva, S. V. *Chem. Sci.* **2013**, *4*, 1939–1949.
- (2) (a) Ishikawa, N.; Sugita, M.; Ishikawa, T.; Koshihara, S.-y.; Kaizu, Y. *J. Am. Chem. Soc.* **2003**, *125*, 8694–8695. (b) Rinehart, J. D.; Fang, M.; Evans, W. J.; Long, J. R. *Nat. Chem.* **2011**, *3*, 538–542. (c) Habib, F.; Murugesu, M. *Chem. Soc. Rev.* **2013**, *42*, 3278–3288.
- (3) (a) Cucinotta, G.; Perfetti, M.; Luzon, J.; Etienne, M.; Car, P.-E.; Caneschi, A.; Calvez, G.; Bernot, K.; Sessoli, R. *Angew. Chem., Int. Ed.* **2012**, *51*, 1606–1610. (b) Pointillart, F.; Le Guennic, B.; Golhen, S.; Cador, O.; Maury, O.; Ouahab, L. *Chem. Commun.* **2013**, *49*, 615–617. (c) Long, J.; Vallat, R.; Ferreira, R. A. S.; Carlos, L. D.; Almeida Paz, F. A.; Guaria, Y.; Larionova, J. *Chem. Commun.* **2012**, *48*, 9974–9976.
- (4) Zheng, Y.-Z.; Zhou, G.-J.; Zheng, Z.; Winpenny, R. E. P. *Chem. Soc. Rev.* **2014**, *43*, 1462–1475.
- (5) (a) Woodruff, D. N.; Winpenny, R. E. P.; Layfield, R. A. *Chem. Rev.* **2013**, *113*, 5110–5148. (b) Rinehart, J. D.; Long, J. R. *Chem. Sci.* **2011**, *2*, 2078–2085.
- (6) Sabbatini, N.; Guardigli, M.; Lehn, J.-M. *Coord. Chem. Rev.* **1993**, *123*, 201–228.
- (7) Cotton, S. *Lanthanide and Actinide Chemistry*; John Wiley & Sons: West Sussex, U. K., 2006.
- (8) Alexandropoulos, D. I.; Mowson, A. M.; Pilkington, M.; Bekiari, V.; Christou, G.; Stamatatos, Th. C. *Dalton Trans.* **2014**, *43*, 1965–1969.
- (9) For a $\text{Ti}^{\text{IV}}/\text{nd}^{2-}$ cluster, see: Wallace, W. A.; Potvin, P. G. *Inorg. Chem.* **2007**, *46*, 9463–9472.
- (10) Stamatatos, Th. C.; Christou, A. G.; Mukherjee, S.; Poole, K. M.; Lampropoulos, C.; Abboud, K. A.; O’Brien, T. A.; Christou, G. *Inorg. Chem.* **2008**, *47*, 9021–9034.
- (11) Boudalis, A. K.; Dahan, F.; Bousseksou, A.; Tuchagues, J.-P.; Perlepes, S. P. *Dalton Trans.* **2003**, 3411–3418.
- (12) Alvarez, S.; Alemany, P.; Casanova, D.; Cirera, J.; Lluell, M.; Avnir, D. *Coord. Chem. Rev.* **2005**, *249*, 1693–1708.
- (13) Bartolomé, J.; Filoti, G.; Kuncser, V.; Schinteie, G.; Mereacre, V.; Anson, C. E.; Powell, A. K.; Prodius, D.; Turta, C. *Phys. Rev. B* **2009**, *80*, 014430–16.
- (14) (a) Lehn, J.-M. *Angew. Chem., Int. Ed.* **1990**, *29*, 1304–1319. (b) Binnemans, K. *Chem. Rev.* **2009**, *109*, 4283–4374. (c) Bekiari, V.; Lianos, P. *Adv. Mater.* **2000**, *12*, 1603–1605.